



Fermi National Accelerator Laboratory

FERMILAB-Conf-98/107-E

D0

The Forward Proton Detector at D0

Gilvan A. Alves

For the D0 Collaboration

*Centro Brasileiro de Pesquisas Fisicas
Rua Xavier Sigaud 150, 22290-180, Rio de Janeiro, RJ, Brasil*

*Fermi National Accelerator Laboratory
P.O. Box 500, Batavia, Illinois 60510*

April 1998

Published Proceedings of *Lishep 98 - Workshop on Diffractive Physics*,
Rio de Janeiro, Brazil, February 16-20, 1998

Disclaimer

This report was prepared as an account of work sponsored by an agency of the United States Government. Neither the United States Government nor any agency thereof, nor any of their employees, makes any warranty, expressed or implied, or assumes any legal liability or responsibility for the accuracy, completeness, or usefulness of any information, apparatus, product, or process disclosed, or represents that its use would not infringe privately owned rights. Reference herein to any specific commercial product, process, or service by trade name, trademark, manufacturer, or otherwise, does not necessarily constitute or imply its endorsement, recommendation, or favoring by the United States Government or any agency thereof. The views and opinions of authors expressed herein do not necessarily state or reflect those of the United States Government or any agency thereof.

Distribution

Approved for public release; further dissemination unlimited.

The Forward Proton Detector at DØ

Gilvan A. Alves^{†*}

Centro Brasileiro de Pesquisas Físicas

Rua Xavier Sigaud 150, 22290-180, Rio de Janeiro, RJ, Brasil

(May 1, 1998)

[†]For the DØ Collaboration

We present the first results of detector R & D done for the proposed Forward Proton Detector at DØ. From a menu of options we have chosen a scintillating fiber based detector with multi-anode photomultiplier readout.

I. PHYSICS MOTIVATION

The interest in diffractive scattering has been growing since the observation of diffractive production of jets, by the UA8 collaboration [1]. This observation came in support of the recently introduced field of hard diffraction, in which the diffractive scattering is accompanied by high transverse momentum objects [2].

In principle such kind of events could be treated in terms of parton language, defining a partonic structure for the exchanged object. Diffractive events can also be characterized by rapidity gaps, regions of the phase space with no particles. This is due to the colorless nature of the exchanged object. Diffractive kinematics are summarized in Fig. 1.

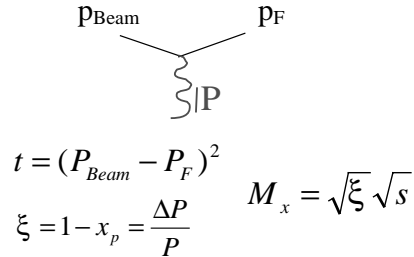
The experimental difficulty in observing these events is that the scattered proton tends to remain in the beam pipe and can not be detected using the typical collider central detectors. For that it is necessary to add special forward particle detectors to the central assembly at very small angles, or large distances from the collision point.

Although rapidity gap techniques give some information on the diffractive event, only the addition of a forward particle detector would allow access to the full kinematics of the scattered particle.

Other motivation for adding a forward particle detector follows:

- The Interest in Hard Diffraction has been growing dramatically due to recent results from HERA (H1, ZEUS) and Tevatron (CDF, DØ).
- For the next 10 years much of this physics can only be done at the Tevatron collider. Diffractive systems with masses greater than $450 \text{ GeV}/c^2$ can be produced at Tevatron compared to only $70 \text{ GeV}/c^2$ at HERA.
- Some processes like diffractive dijet production are well established, but not accurately measured.
- Other processes like hard double pomeron exchange are not yet observed, but are likely to exist.
- There are chances for discovery of new physics, like centauros, glueballs, etc.
- Since there is little data on elastic scattering except at small $|t|$, such a detector could extend our knowledge to the high portion of the $|t|$ spectrum.

*Partially supported by a grant from Capes/Brazil



$$\begin{aligned}
 t &= (P_{Beam} - P_F)^2 \\
 \xi &= 1 - x_p = \frac{\Delta P}{P} \\
 M_x &= \sqrt{\xi} \sqrt{s}
 \end{aligned}$$

FIG. 1. Kinematic variables in diffractive scattering. Here t corresponds to the four-momentum transfer squared, \sqrt{s} is the center of mass energy, x_p is the fractional momentum carried by the scattered proton, and M_x is the diffractive mass.

II. THE FORWARD PROTON DETECTOR

The Forward Proton Detector [3] is a series of momentum spectrometers that make use of machine magnets in conjunction with position detectors along the beam line in order to determine the kinematic variables (t and ξ) of the scattered protons and anti-protons. The position detectors have to operate a few mm from the beam position and have to be moved away during the machine injection time. Special devices called “Roman pots” are designed to house the position detectors allowing for remotely controlled movement with good accuracy. The Roman pots for the Forward Proton Detector are described in a separate work presented at this conference [4]. The greatest challenge for the use of these devices in our case, is the limited space available around the $D\emptyset$ interaction region.

Figure 2 shows a schematic representation of the location of the Roman Pots with respect to the $D\emptyset$ collision point. Spectrometers are labeled with respect to the analyzing magnet used. While the dipole spectrometer has detectors only in the horizontal direction, quadrupole spectrometers have detectors in both horizontal and vertical directions in order to maximize the acceptance.

This layout requires a total of 18 position detectors for both dipole and quadrupole spectrometers. It gives us the ability to trigger on both scattered protons and anti-protons while the hard scattering products are measured using the full $D\emptyset$ detector.

III. DETECTOR GOALS

In order to characterize the hard diffractive events we need to be able to measure its kinematic variables to a good precision. However, external factors like the beam dispersion, uncertainty in beam position, multiple scattering and Roman Pot positioning limit the attainable resolution. Hence a point resolution of about $100\mu\text{m}$ is sufficient for the Forward Proton Detector. Some desirable characteristics for this detector are listed below:

- Overall efficiency close to 100%
- Modest radiation hardness. The detector will be operating at approximately 8σ (σ is the beam standard deviation) from the beam axis, so the expected radiation dose for one year of running is only 0.03 Mrad.
- High Rate capability. The detector needs to be live at every beam crossing.
- Low sensitivity to accelerator background, in particular particle showering along the beam pipe or magnets.
- Small dead area closer to the beam. This is particularly important since the protons are scattered at very low angles, so the detector acceptance is heavily dependent on its position relative to the beam axis.

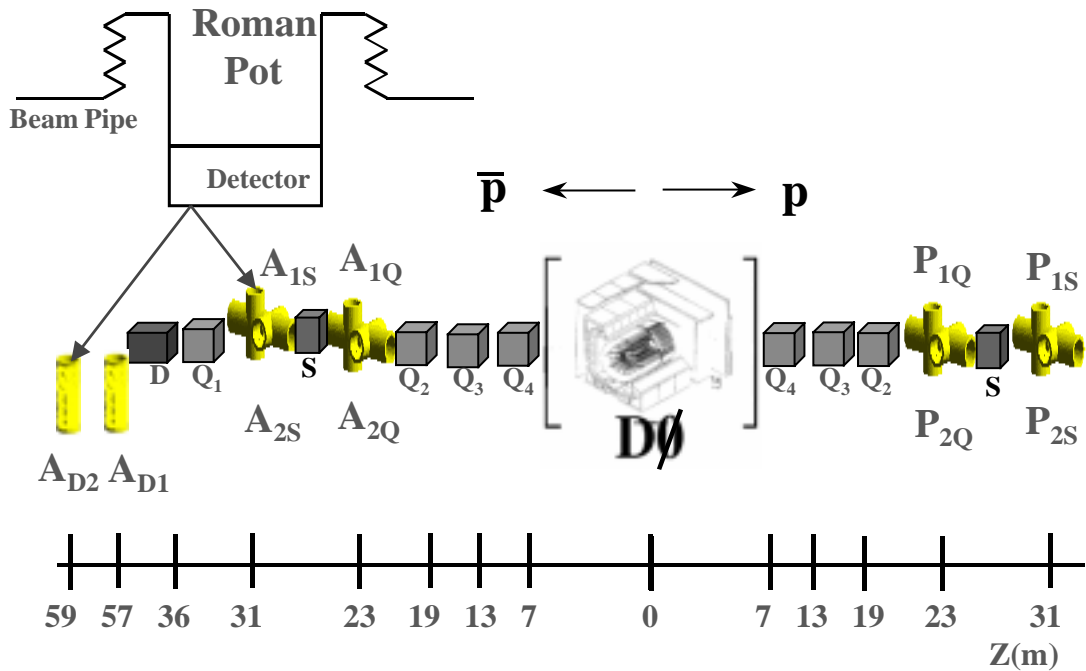


FIG. 2. Schematic placement of the position detectors around the DØ collision hall. The labels A and P represent the anti-proton and proton side detectors respectively, while Q, S and D label the quadrupole, separator, and dipole magnets.

IV. DETECTOR OPTIONS

We have considered several options for the position detector, some of which are listed below:

- Silicon Microstrip Detector
- Microstrip Gas Chamber (MSGC)
- Scintillating Fiber Detector

In Table I we present some of the advantages and disadvantages of each of these detector options.

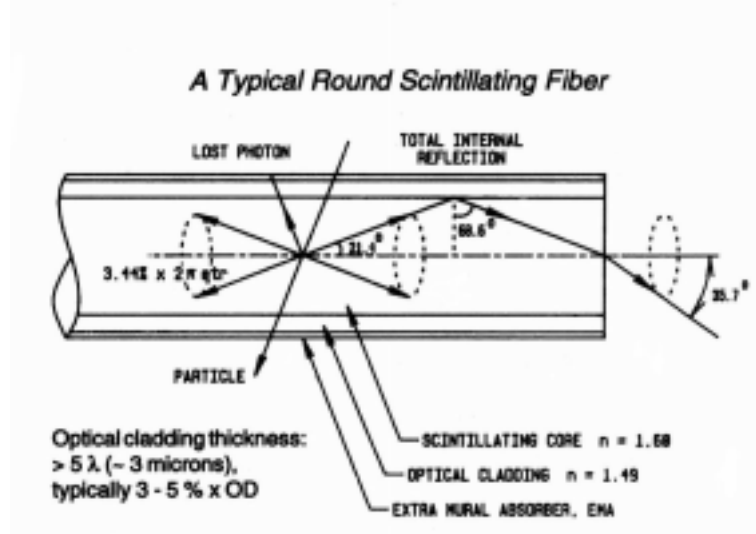
TABLE I. Detector Options for the FPD

Detector	Pro	Con
Silicon	Superior Resolution	Dead Area Trigger
MSGC	Good Resolution	Dead Area
Fiber	Adequate Resolution	Light Output

Silicon microstrip detectors have very good resolution and can operate at high rates, however they have a high cost/channel and problems with dead area at the bottom of the pot (1mm), where acceptance is crucial. Also the readout time for this detector is not fast enough to use it in a Level 1 trigger, which we find necessary in order to reduce the event rates to an acceptable level.

MSGCs suffer from an even worse dead area problem as compared to silicon detectors. Reducing this dead area could be possible, but it would involve considerable efforts in Research and Development (R & D).

Scintillating Fiber Detectors do not present the dead area problem and can be read out using fast devices like photomultiplier tubes or photodiodes. A drawback of these detectors is the small light yield obtained from fibers that have a small enough diameter to give the desired position resolution. This can be seen from equation (1), which expresses the light yield as a function of several parameters, including the length of the fiber material traversed by the particle.



LightYield(Y)

$$Y = Y_0 \cdot F \cdot A \quad (1)$$

$Y_0 \Rightarrow$ Initial Yield

$F \Rightarrow$ Trapping Efficiency ≈ 0.04

$A \Rightarrow$ Fiber Attenuation

$$Y_0 = \frac{dE}{dx} \cdot \Delta x \cdot V \cdot \left(\frac{C_s}{\Delta E_{eff}} \right)$$

where

Δx is the effective pathlength of the particle in the fiber

V is the fractional volume of the fiber core

C_s is the sci. fiber light conversion efficiency

ΔE_{eff} is the effective energy to generate a photon

This problem can be overcome by the use of very efficient photon detection devices, like the Visible Light Photon Counter (VLPC) [5], the Avalanche Photo Diode (APD), the Image Intensifier with CCD readout, and the Multi Anode Photomultiplier (MAPMT) among others. A comparison of the Quantum Efficiency (light to charge conversion) between these devices is given below.

Device	Quantum Efficiency
VLPC	($\approx 80\%$)
APD	($\approx 70\%$)
Image Intensifier + CCD	($\approx 20\%$)
MAPMT	($\approx 20\%$)

APDs are still in a development stage, especially for our application, which requires multiple channels in a single chip. Image Intensifiers with CCD readout cannot operate at the high rate needed by our detector. VLPCs, which were developed within the DØ collaboration, are by far the best option in terms of quantum efficiency, but the cost and complications of the cryogenics associated with it led us to the far simpler MAPMT. These devices have a reasonable sensitivity, high gain and can be operated at very high rates. We have chosen to use Hamamatsu H6568 16 channels MAPMT, which has single photoelectron (PE) sensitivity and good gain stability between channels.

Within the fiber framework we have investigated several options as detection elements:

- A thin piece of scintillator tile connected to clear fibers for readout.
- A thin piece of scintillator tile connected to wavelength shifting fibers for readout.
- Scintillating fiber bundle straight from the detector area to the MAPMT.
- Scintillating fiber bundle connected to clear fiber for readout.

We have decided to use square fibers as opposed to round due to the fact that the former type gives an increase of about 20% in the light output. We use 0.8mm square fibers, giving about $80\mu\text{m}$ point resolution, which is close to the desired value. The fibers were bundled in groups of four, since earlier studies have indicated that such an arrangement would give around 10 photoelectrons. In all cases one end of the detector element was aluminized to increase the light yield. Figure 3 shows a schematic drawing of the test setup used to compare different detection elements. All tests were done using $^{90}_{38}\text{Sr}$ and $^{106}_{44}\text{Ru}$ radioactive sources collimated to the fiber dimension. A single channel of the Hamamatsu H6568 16 channel MAPMT read out the four fiber bundles. Single PE calibration was done using a short pulse through a blue LED.

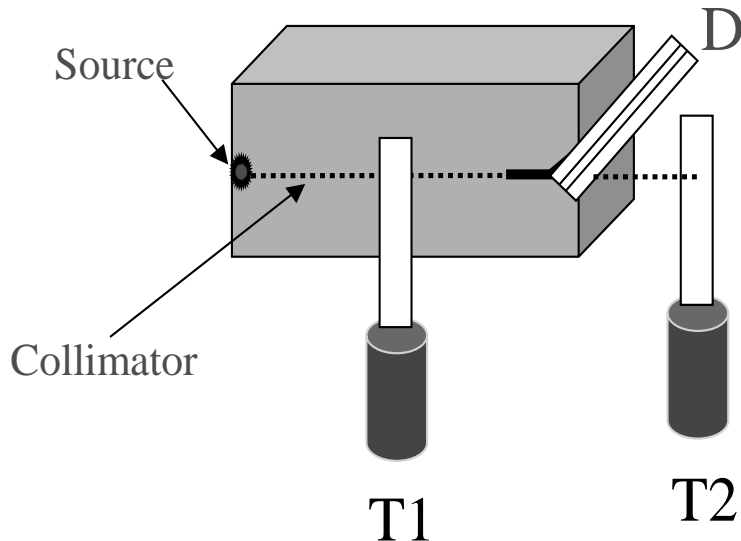


FIG. 3. Source setup for testing FPD detector elements (D). T1 and T2 are trigger scintillators. D is readout by a MAPMT (see text).

Results show a clear advantage in using scintillating fibers in comparison to a scintillator tile. This could be due to a possible lower trapping efficiency for the thin tile. We have also noticed that the thin tiles are very fragile, often developing several fractures even being handled with extreme care. Figures 4, 5 and 6 show the integrated charge for each of the options tested.

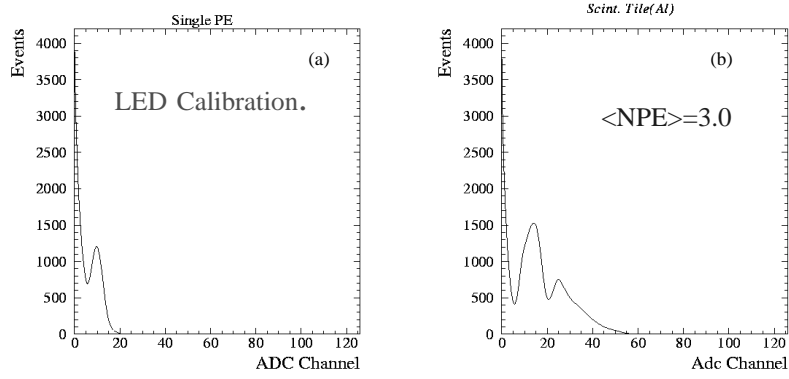


FIG. 4. Integrated charge from MAPMT readout of detector elements. (a) shows the LED calibration of the single photoelectron peak. (b) is the charge distribution for a thin scintillator tile plus clear fiber as waveguide.

Figure 5 (b) shows the net effect of having the aluminized end of the detector cut at a 45° angle. Having the fiber planes oriented at this angle (U, V planes instead of X, Y) would decrease the radius for the fiber bending, resulting in a more compact Roman Pot with the additional advantage of avoiding complicated pressure compensating mechanisms for this device. We can see that the effect of plane orientation is minimal.

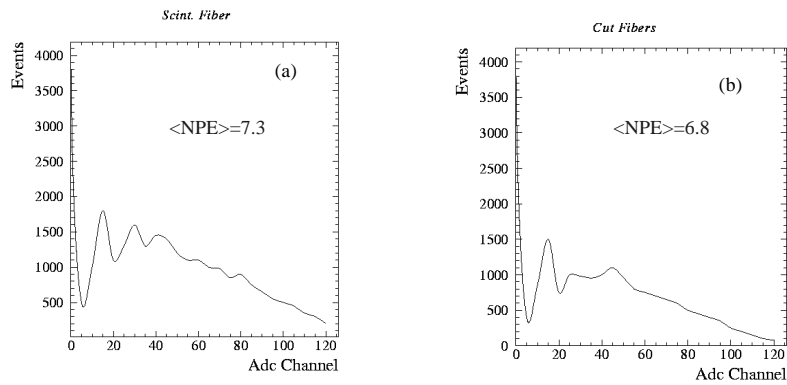


FIG. 5. Integrated charge from MAPMT readout of detector elements. (a) shows the distribution from four 0.8mm thick by 50cm long scintillating fibers aluminized at one end, and (b) shows the same arrangement but with the aluminized end cut at a 45° angle with respect to the fiber axis.

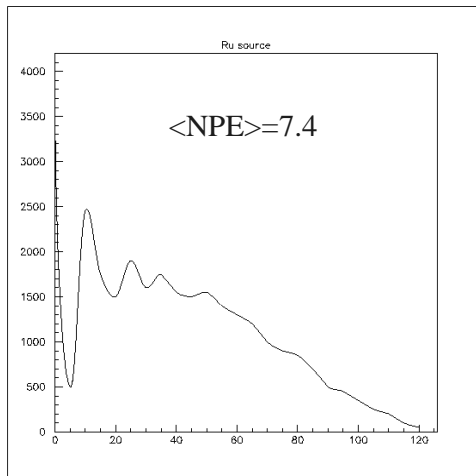


FIG. 6. Integrated charge distribution from MAPMT readout of a detector element consisting of 4 scintillating fibers 0.8mm thick by 5cm long cut at a 45° angle in one side and glued to 50cm long clear fibers as a waveguide.

The setup using scintillating fibers spliced to clear fibers was chosen bearing in mind the effects of the halo background in the scintillating fibers alone, and also a slight decrease in the optical cross-talk with this setup. A comparison between Fig.6 and Fig.5 (b) shows that the scintillating plus clear fiber combination actually improves the light output due to the shorter attenuation length of the smaller scintillating fiber. Preliminary efficiency measurements done using the chosen setup range from 90-95%. This measurement does still have a residual photon background from the radioactive source and we are working on a cosmic ray setup to solve this problem. We have also detected a dependence of this result on the cutting, mirroring and splicing procedures, which have to be monitored carefully. The final detector configuration is shown in Fig. 7. There will be 6 planes in 3 views (U, V and X) in order to minimize ghost hit problems. The fibers will be mounted on a thin plastic frame, amounting to 112 channels per detector and a total of 2016 channels in all spectrometers. Each channel corresponds to 4 scintillating fibers, which fits nicely in the 4mm x 4mm-pixel size of the H6568 MAPMT. A total of 7 MAPMT will be needed for each detector, which represents the major component in the detector cost. This detector will allow us to make high-statistics and precise measurements of hard as well as inclusive diffractive processes, studying the dependence of these processes on kinematic variables. The combination of that with measurements in the central $D\bar{O}$ detector will allow us to distinguish between different models for the pomeron structure.

V. CONCLUSIONS

After considering several alternatives a scintillating fiber based detector with MAPMT readout was chosen as the best option for the FPD, considering all the aspects of acceptance, costs, radiation hardness and trigger capabilities. A prototype detector is being built at FNAL for resolution studies, and will be tested using a cosmic ray and, if available, a test beam setup. The FPD will add to the already existing diffractive physics program of $D\bar{O}$, being completely integrated to the existing detector.

The field of Hard Diffraction is in clear need of more precise data for a better understanding of the diffractive phenomena, and the FPD will certainly help to achieve this goal.

The arrangement of quadrupole and dipole spectrometers that we have chosen will extend the kinematic range of previous detectors, helps us in a better understanding of alignment and background issues, and could also be used for luminosity measurements.

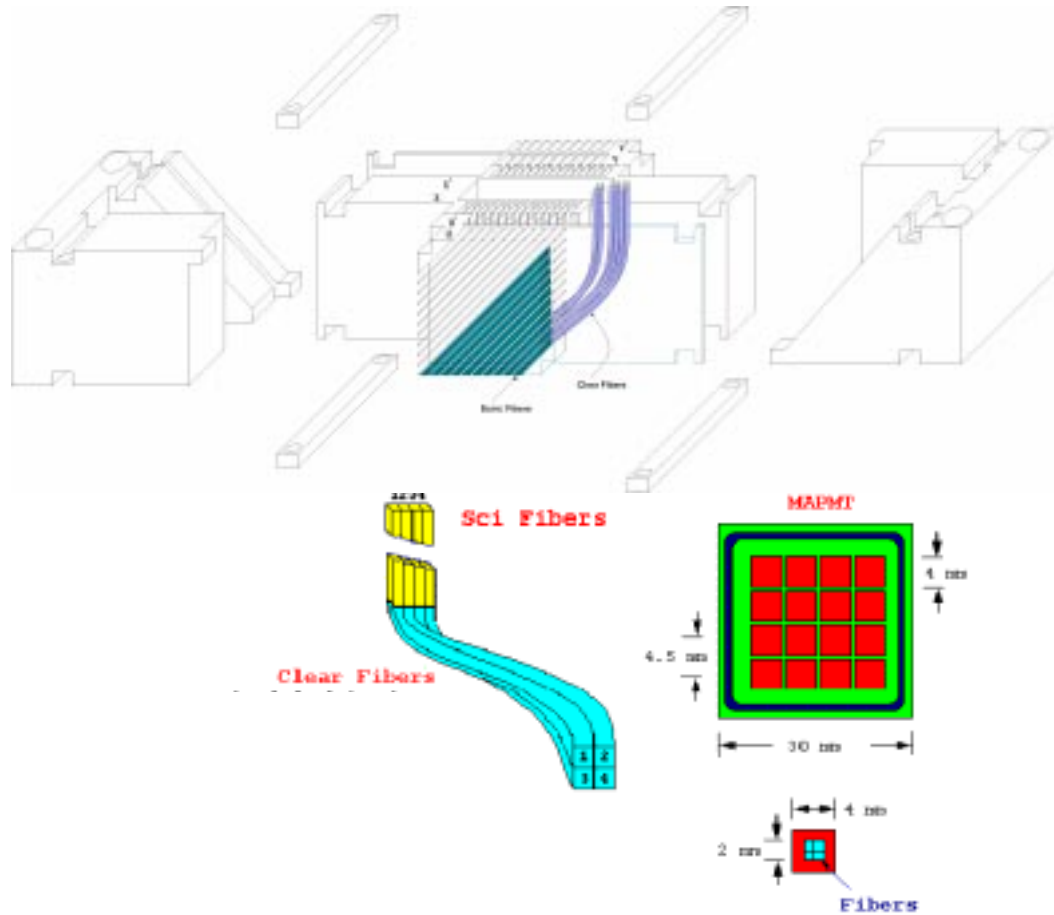


FIG. 7. Proposed design for each FPD detector. Also shown are the frames for fiber alignment and the fiber to photomultiplier interface.

-
- [1] R. Bonino et al.(UA8 Collaboration)Phys. Lett. 211B (1988) 239.
 - A. Brandt et al.(UA8 Collaboration) Phys. Lett. 297B (1992) 417.
 - [2] G. Ingelman and P. Schlein Phys. Lett. 152B (1985) 256.
 - [3] A. Brandt et al., "A Forward Proton Detector at DØ", FERMILAB- Pub-97/377.
 - [4] H. da Motta, "The FPD Roman Pot design", This conference proceedings.
 - [5] D. Adams et al., IEEE Trans.Nucl.Sci.,43 (1996) 1146.